TILL COMPOSITION ACROSS THE MELIADINE TREND, RANKIN INLET AREA, KIVALLIQ REGION, NUNAVUT

Geological Survey of Canada Open File 3747

November 2000

ISABELLE McMARTIN

Contribution to the

NATMAP WESTERN CHURCHILL PROJECT

NATMAP CARTNAT

Western Churchill Project

Canada's National Geoscience Mapping Program

Le Programme National de Cartographie Géoscientifique du Canada

Natural Resources Canada

Ressources Naturelles Canada

Canada

TABLE OF CONTENTS

INTRODUCTION	4
LOCATION	4
REGIONAL GEOLOGY	5
METHODOLOGY	12
Field procedures	12
Laboratory procedures	15
QA/QC	19
RESULTS AND DISCUSSION	21
Till matrix colour and texture	21
Till lithology	23
Till matrix mineralogy	24
Till matrix geochemistry	25
Heavy mineral geochemistry	30
Visible gold grains	31
CONCLUSIONS	31
ACKNOWLEDGEMENTS	35
REFERENCES	35
APPENDICES	41
DIGITAL DATA	

Digital copy of report (PDF format) and Appendices I-XV (Excel and PDF) are available on CD-ROM from GSC Bookstore, 601 Booth Street, Ottawa, Ontario, K1A 0E8, (613) 995-4342, Internet: gsc_bookstore@gsc.emr.ca.

FIGURES

1.	Location map of study area in the Kivalliq Region	6
2.	Detailed location map	7
3.	Bedrock geology map	8
4.	Dispersal of Dubawnt erratics and distribution of red till	10
5.	Generalized surficial geology map	11
6.	Ice flow indicator map	13
7.	Analytical scheme	16
8.	Turbic cryosols	22
9.	Au-As relationship in <63 µm of till	29
10.	As in HMCs versus As in <63 µm of till	29
11.	Au in HMCs versus Au in <63 µm of till	32
12.	Au-As relationship in HMCs	32
13.	Au grains versus Au in <63 µm of till	33

APPENDICES

I.	Field stations	41
II.	Samples	60
III.	Erosional ice flow indicators	81
IV.	Pebble lithological composition	90
V.	Carbonate mineralogy	107
VI.	Geochemistry < 0.002 mm, ICP-AES	122
VII.	Geochemistry < 0.063 mm, ICP-AES	184
VIII.	Geochemistry < 0.063 mm, INAA	238
IX.	Au < 0.063 mm, Fire assay - ICP-AFS	259
X.	Geochemistry < 0.063 mm of HMC, ICP-AES	262
XI.	Au < 2 mm of HMC, Fire assay and INAA	274
XII.	Au grain counts	278
XIII.	Grain size distribution	303
XIV.	Physical tests	312
XV.	Analytical Quality Control	317

INTRODUCTION

The Western Churchill Province of the Canadian Shield in south-central Nunavut (Kivalliq Region) is a region with high potential for base and precious metal deposits. Mineral exploration and prospecting started nearly 70 years ago over the AEnnedai-Rankin@ greenstone belt (Wright, 1967). A suite of geophysical and geochemical techniques, including drift prospecting (i.e., Shilts, 1973; Ridler and Shilts, 1974; Shilts and Wyatt, 1989; Klassen and Knight, 1996), have been used for mineral exploration. In recent years, several major gold occurrences hosted by the Rankin Inlet Group have been discovered along the Meliadine Trend, 25 km north of Rankin Inlet (Armitage et al., 1993; Miller et al., 1995; Carpenter and Duke, 1999). The Meliadine Trend forms a 65 km long linear aeromagnetic anomaly and extends >65 km west from Hudson Bay. A major part of this highly prospective area is covered by a thick blanket of glacial sediments. As part of the Western Churchill National Mapping Program (NATMAP), a surficial geological and geochemical mapping project was designed by the Geological Survey of Canada to assist mineral exploration along the Meliadine Trend. The specific objectives of the project are to 1) provide a Quaternary geological framework for drift prospecting, 2) determine the signature of the known gold occurrences in glacial sediments and propose a glacial dispersal model for the region, 3) supply a surficial materials database that would serve as a baseline for environmental assessment for future development, and 4) produce surficial geology maps at 1:50 000 scale (5 NTS sheets).

This open file presents data collected by the Geological Survey of Canada regarding till provenance and geochemistry for regional samples and for samples collected near selected zones of mineralization. Data on the composition and physical characteristics of glaciofluvial, glaciomarine and marine sediment samples are included, as well as erosional ice flow indicators and field site descriptions. A summary of the regional geology is presented together with an extensive description of field and laboratory methods. Results are discussed briefly for till composition only. A full discussion will be presented in further reports and papers, specifically regarding the signature of the known gold occurrences in till, glacial transport and implications for drift prospecting, and field methods in permafrost terrain, including the examination of the effects of surface weathering and marine reworking on till geochemistry.

LOCATION

The area studied is located in the Kivalliq Region of Nunavut along the northwestern side of Hudson Bay, approximately 480 km north of Churchill, Manitoba, and includes the town of Rankin

Inlet (Fig. 1). The only major route outside Rankin Inlet is a gravel road that reaches the Meliadine River 10 km to the north (Fig. 2). The area covers approximately 2,800 km^2 and is bounded by latitudes 62°45' and 63°15' N and longitudes 91° and 93° W, an area that covers the Archean Rankin Inlet Greenstone Belt (Tella, 1994). It spans the following 1:50 000 scale National Topographic Series maps: Falstaff Island (55 J/13), Scarab (55 J/14), Rankin Inlet (55 K/16), Meliadine Lake (55 N/1), and APeter Lake@ (55 N/2). Rankin Inlet is the site of the only mine brought into production in the entire region to date, the North Rankin Nickel Mines Limited, which was closed in 1962 due to the lack of ore.

REGIONAL GEOLOGY

Bedrock geology and mineralization

The Archean (ca. 2.66 Ga.) Rankin Inlet Greenstone Belt (Tella, 1994, 1995) covers about 65% of the study area (Fig. 3). It includes essentially the Rankin Inlet Group (Tella et al., 1986), a metavolcanic-metasedimentary sequence deformed and metamorphosed to greenschist grade. The Rankin Inlet Group is composed of sheared and carbonatized massive and pillowed mafic volcanic flows (1), felsic volcanics (2), interflow sediments (3), mainly greywacke and quartz-magnetite iron formation, and minor mafic and felsic tuffs, pyroclastics, volcanic breccia and gabbro sills (Tella et al., 1997). The higher metamorphic grade equivalents of the greenstone belt rocks are exposed north of the Rankin Inlet Group and comprise gneiss and minor remnants of banded iron formation (4). Archean and/or Paleoproterozoic layered gneiss and migmatite border the rest of the greenstone belt (5). Several compositionally distinct Archean and/or Early Proterozoic granitoid plutons are found throughout the area (6,7,9). Proterozoic sediments correlative with the Hurwitz Group discontinuously overly the sequence (8).

The Meliadine Trend is characterized by a regional pervasive structural zone (Pyke Fault Zone) located at the southern edge of oxide iron-formation within the Rankin Inlet Group (Miller et al., 1995; Carpenter and Duke, 1999). Active gold exploration in the region is focused on the oxide facies iron formation and associated sediments, as well as on high strain zones at volcanic-sediment contacts associated with deformation along and near the Pyke Fault (Tella et al., 1992; Armitage et al., 1993; Miller et al., 1995; Carpenter and Duke, 1999, 2000). All significant gold occurrences are located near but north of the ESE-striking Pike Fault. Both types of gold mineralization are characterized by coarse grained arsenopyrite (Armitage et al., 1993), but gold does not always correlate with arsenic (Miller et al., 1995; James et al., 2000; J. Kerswill, pers.

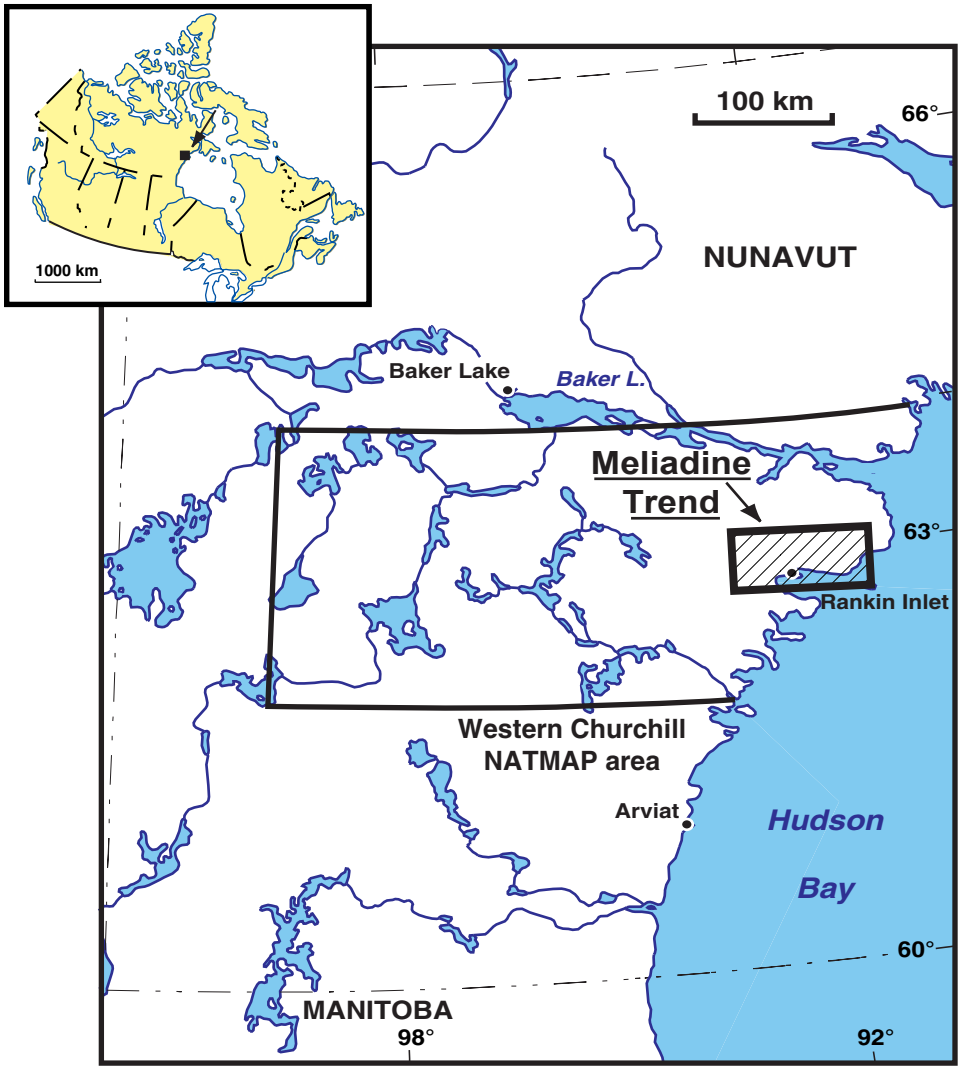

Figure 1. Location map of study area in the Kivalliq Region of Nunavut. The Western Churchill NATMAP area is also shown.

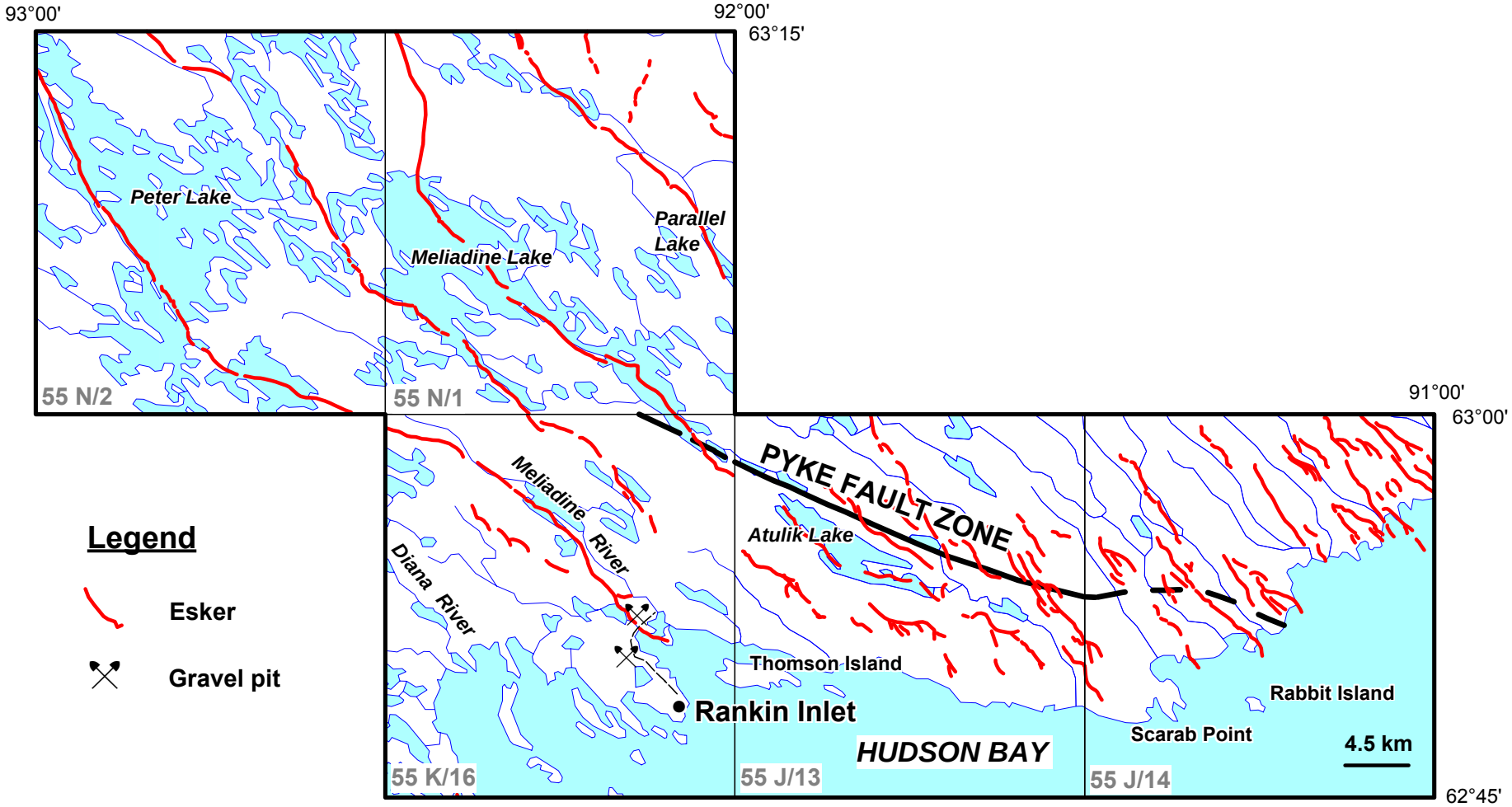

Figure 2. Detailed location map of study area showing hydrology, eskers, geographic locations and NTS map sheets. The location of the Pyke Fault Zone is approximate.

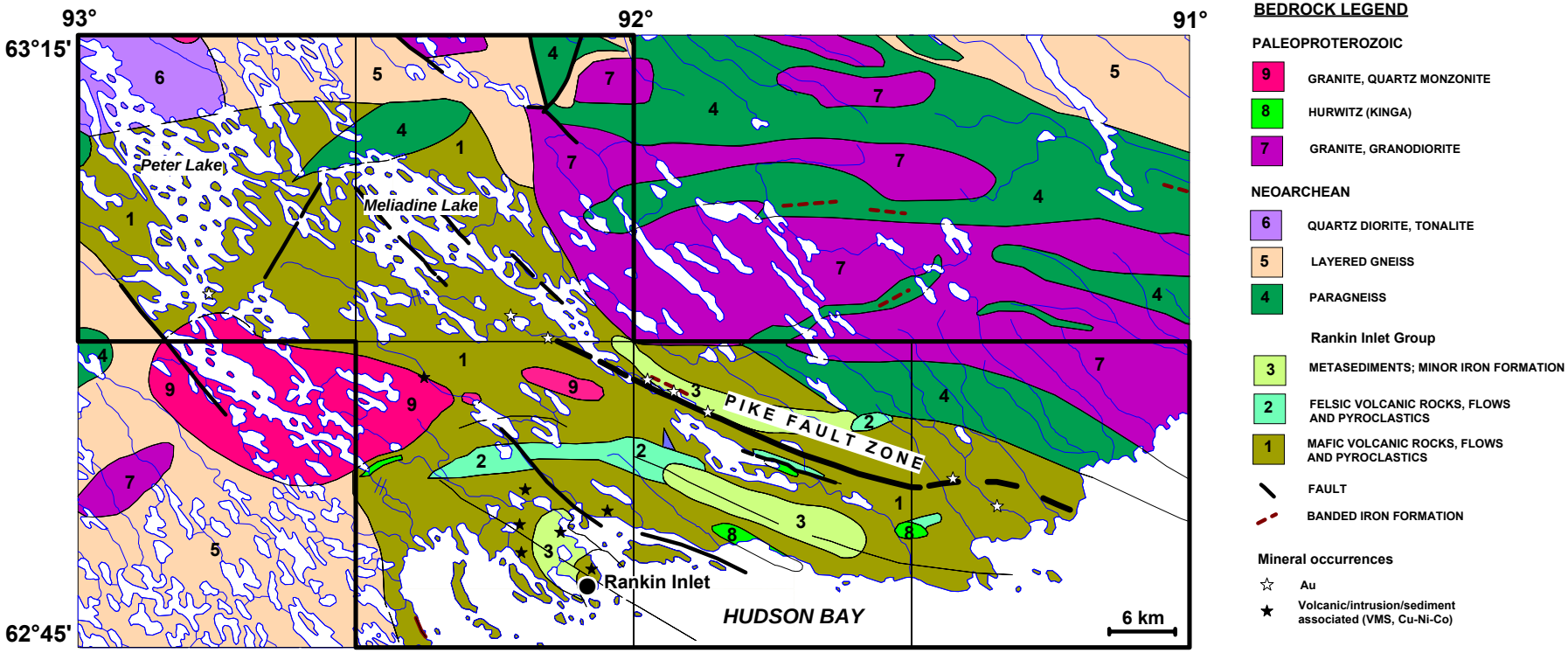

Figure 3. Bedrock geology map (from Tella et al., 1997).

comm.). In the oxide iron formation, for example at the Discovery Zone, the visible gold is associated with pyrrhotite, arsenopyrite, pyrite, and minor chalcopyrite (Armitage et al., 1993) and is concentrated in individual hinge and limb segments of the folded iron formation. Gold mineralization related to high strain zones differs from iron-formation hosted gold mineralization in deformation style and silicate, carbonate, sulphide, and gold composition (Miller et al., 1995). At AWesmeg@, gold is associated with arsenopyrite with pyrite, chalcopyrite, pyrrhotite and galena. Free gold in both types of mineralization also occurs intergranular to sulphides and as fracture fillings, inclusions and coatings, dissiminated, and in sulphide-bearing carbonate-quartz veins.

Glacial geology

During the last glaciation, Keewatin Sector ice of the Laurentide Ice Sheet, flowing in a southeasterly direction, deposited a sandy till containing a mixture of local and exotic debris over the Kivalliq region. The Meliadine area lies at the edge of the southeastward Dubawnt glacial dispersal train (Shilts et al., 1979), hence surface till clast composition and reddish color reflect the incorporation of far-travelled debris in the southwest part of area, but not in the northeast (Fig. 4). Hand dug pits, small natural sections and drill hole data indicate that till is the predominant surficial sediment in the area (Fig. 5) and that it forms the bulk of streamlined landforms, ribbed moraines, DeGeer moraines and hummocky moraines. Following deglaciation, between 7 and 6 ka BP (^{14}C), marine submergence resulted in the deposition of a discontinuous, thin veneer of marine sediments over the glacial landforms. Concurrent isostatic rebound caused a rapid rise in the land surface, and as the land emerged, till and marine sediments were variably reworked by wave and current action in the Tyrrell Sea.

The Meliadine Lake and Peter Lake map sheets (55N/1 and N/2) are dominated by thick till (<25 m), commonly drumlinized or ribbed, and weakly reworked by the postglacial sea. Only the tops of the landforms are developed into small marine terraces forming distinctive gravel caps. Till is thinner or absent in the northwest part of the Meliadine Lake map area (55N/1) underlain by intrusive rocks. Along the coast, till is prevalent above 30 m a.s.l. in the Rankin Inlet map area (55K/16) and above 60 m a.s.l. east of Atulik Lake (55J/13 and J/14). In these areas, topographic lows are commonly filled with a veneer of marine sands and silts and the tops of landforms are locally reworked into beaches, terraces and spits. Below the till-dominated areas, marine littoral sand and gravel, nearshore and tidal sands fill lowland between bedrock outcrops. Till, where preserved, is generally thin and wave-washed. Four major continuous trunk eskers with tributaries

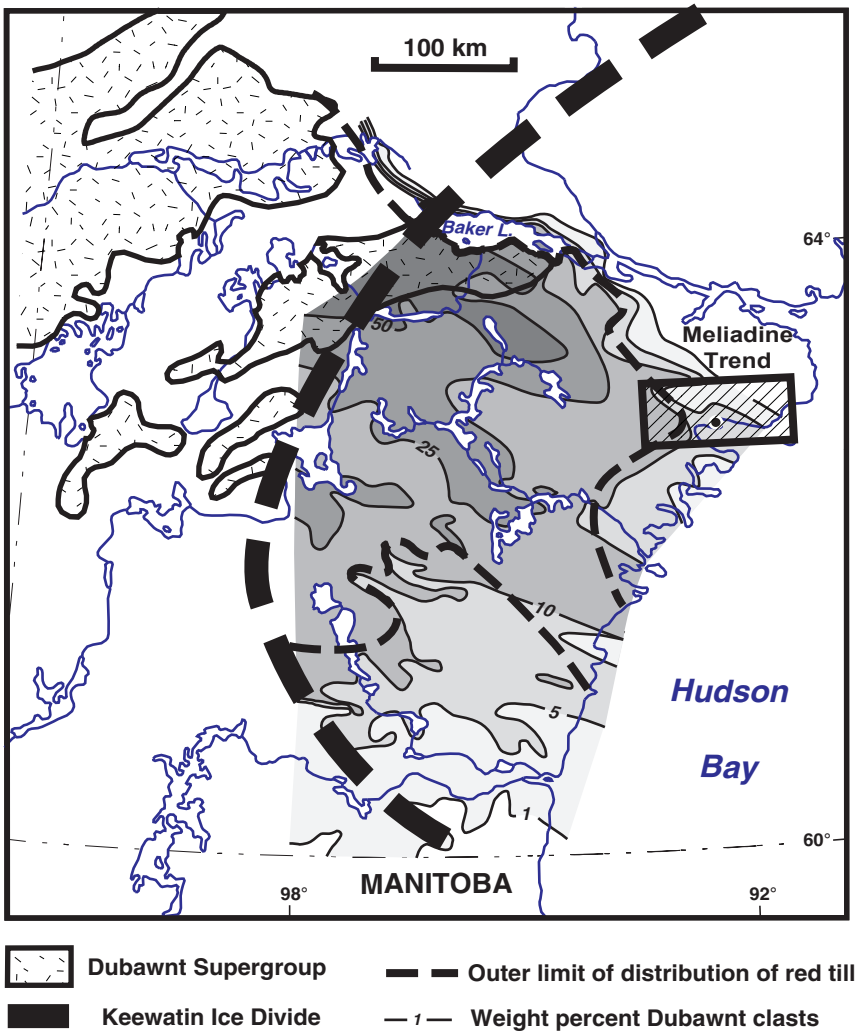

Figure 4. Dispersal of Dubawnt Supergroup erratics (2 to 6 mm fraction of till) and distribution of red till (from Shilts et al., 1979). The central axis of the Keewatin Ice Divide is shown as a thick dashed line.

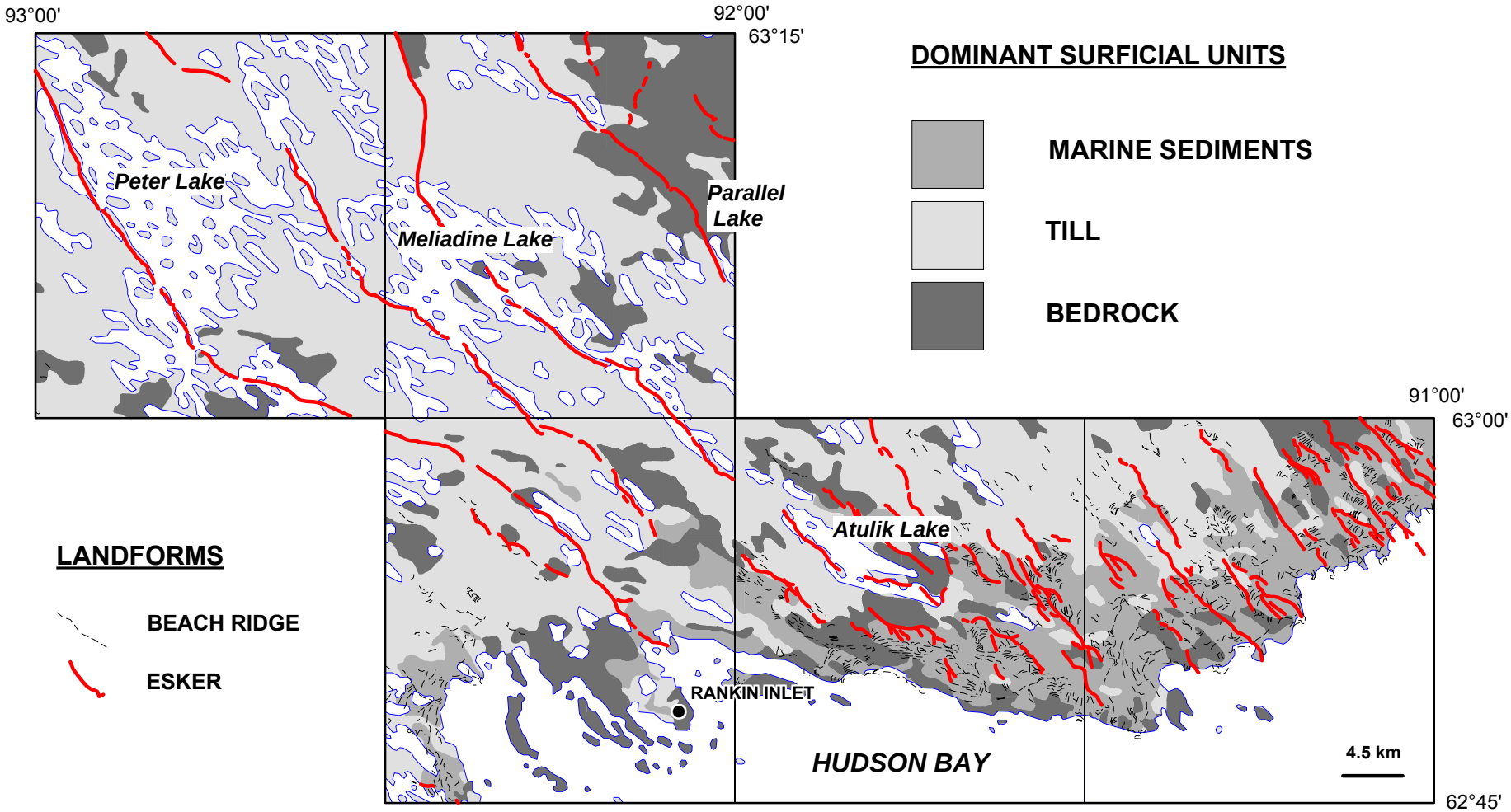

Figure 5. Generalized surficial geology map showing dominant surficial units, beach ridges and eskers (modified from Aylsworth et al., 1981a, 1981b, 1984).

joining at near 90° angles from the north traverse the area from west to east: Peter Lake, Sic Sic, Meliadine Lake, and Parallel Lake eskers. These eskers are commonly beaded and aligned within major topographic lows. East of Atulik Lake, eskers are numerous, closely spaced, discontinuous, and extensively reworked by marine action. Other minor surficial units in the study area include undifferentiated alluvium and fine grained marine sediments, shallow peatlands, and glaciomarine diamictons.

Ice flow indicators (rf. Field procedures section) recorded on bedrock across the area trend to the southeast, parallel to the long axes of lakes, streamlined landforms and roches moutonnées (Fig. 6). Directions shift slightly from west to east, from an average of 131° in the Peter Lake map area (55N/2) to 147° in the Scarab map sheet (55J/14). Two older regional ice flows mapped in the Kivalliq Region (McMartin and Henderson, 1999) have also been recognized in the area : 1) striations indicating a more south-southeasterly (149° to 152°) flow and preserved on the lee-side of the regional southeast trending indicators were observed at a few sites in the western part of the area and south of Rankin Inlet, and 2) well-preserved surfaces with striations indicating an older flow to the east-southeast (114° to 122°) were commonly found along the coast east of Rankin Inlet on recently emerged bedrock outcrops. In the vicinity of the large eskers (<4 km), the youngest ice flow indicators are found at right angle or oblique to the esker direction. Within these corridors, the regional southeastward trending striae and drumlins are generally preserved. At several sites however, particularly to the north of the eskers, DeGeer moraines, and occasionally ribbed moraines, are reoriented obliquely to the SE trending drumlins. These relationships suggest redirection of ice towards the esker ridge near the ice margin (i.e. Veillette, 1986).

METHODOLOGY

Field procedures

Surficial mapping and till sampling were completed during the summers of 1997 through 1999. Access was by helicopter, boat and foot traverses, from Rankin Inlet and from mineral exploration camps (Atulik Lake, Meliadine Lake and Peter Lake). Nearly 545 sites were visited and are described in Appendix I.

Over 220 surface glacial sediment samples (3 kg), mainly till, were collected from active mudboils at an average spacing of 4 km and an average depth of 30 cm. In the vicinity of selected gold occurrences, 80 more till samples were collected. For means of comparison, till samples were

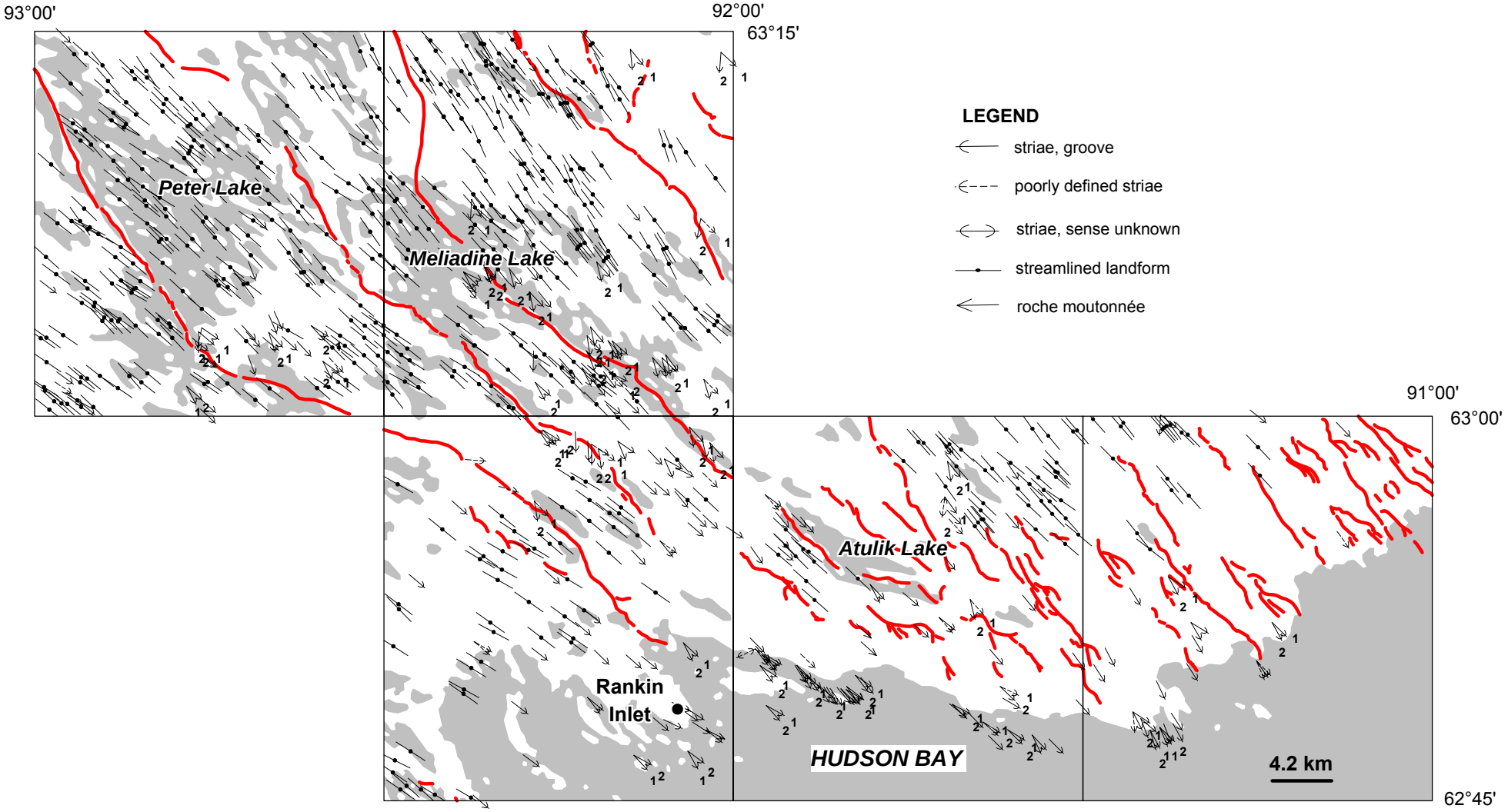

Figure 6. Erosional ice flow indicators measured in the study area (1 = oldest). Streamlined landforms and eskers were taken from Aylsworth et al. (1981a, 1981b, 1984).

classified in the field according to their degree of weathering, reworking by the Tyrrell sea or incorporation of marine sediments through periglacial activity. Most of the till samples fell in Class I when they were collected from fresh mudboils with little sign of oxidation (i.e. Fe-staining), no organic cover and no marine shells. Class I samples were found throughout the area, mainly by photointerpretation prior to sampling, even in the coastal strip of marine sediments. About one third of the samples were slightly oxidized or contained some organic matter and were classified as Class II samples. Class III samples were oxidized (Fe-staining and rotten clasts) and/or contained organic matter and abundant marine shells. Class I and class II tills were preferentially sampled for drift prospecting purposes. About 50 large bulk till samples (10 kg) were collected for gold grain counts, mineralogical and size partitioning studies, heavy mineral geochemistry, and indicator mineral analysis. 36 large esker sediment samples were collected along the Peter Lake esker, and parts of the Meliadine Lake esker where it crosses the Pyke Fault Zone. Shallow soil profiles and mudboils developed in till and marine sediments were sampled in detailed down to permafrost to characterize weathering profiles. The top organic-rich layer (humus) of the soil profiles was also collected. A discussion of results for the esker sediment and profile samples will be presented elsewhere. Sample locations and descriptions are presented in Appendix II together with maps showing sample location (by type) and till sample (by class).

The orientation and relative ages of nearly 275 erosional ice flow indicators were measured from 187 sites. Indicators included striations, grooves, rat tail striae, crescentic gouges and fractures, chattermarks, and roches moutonnées. Measurements were commonly taken on clean lake shoreline outcrops and on flat-lying surfaces to avoid influence by local topography. Outcrops recently cleaned of drift along the coast because of high isostatic uplift rates in the area were ideal sites for observing well preserved striations. The sense of ice flow movement was derived from rat tails, crescentic features, chattermarks and roches moutonnées where present, or from stoss and lee topography. Relative ages of striated facets were interpreted based on the following criteria: a) a set located in a lee-side position relative to another, is usually older, b) a set found only on the top part of an outcrop will have been formed by the youngest movement, c) a set preserved only in depressions and other low positions is interpreted as older, and d) a deeper set (groove) is usually older than a finer set (microstriae). The location and description of erosional ice flow indicators are presented in Appendix III together with ice flow indicator maps.

Laboratory procedures

Sample preparation and analytical procedures for till samples are summarized in Figure 7. About half of a 2 kg split of till and esker sediment samples was wet-sieved to collect the 4-8 mm fraction for lithological analysis. Pebbles were visually examined using a binocular microscope (maximum 250 clasts) and lithologies were divided into Dubawnt Supergroup, Rankin Inlet Group (volcanics, sediments, iron formation), granitoids, and Paleozoic carbonates. Results were calculated by weight % of the total sample and are presented in Appendix IV. Proportional dot maps and descriptive statistics for each major lithological group have been compiled for till and esker sediment samples separately and are included in Appendix IV. Intervals for all maps presented in the Appendices were defined from basic statistics (50, 75, 90, 95, 98, 99,100th percentile). Values below detection limit were assigned 2 detection limit value for the purpose of calculations.

The other half of the 2 kg split of all samples was air-dried and dry-sieved using a stainless steel 230 mesh screen to obtain the <0.063 mm fraction. About 1 g of this fraction (till samples only) was analysed for carbonate mineralogy using the Chittick method at the GSC Sedimentology Laboratory (Dreimanis, 1962). The procedure determines the concentrations of calcite and dolomite based on the different reaction rates of those minerals in hydrochloric acid. The results are presented in Appendix V as weight % calcite, weight % dolomite, weight % total carbonates, and calcite/dolomite ratios. Maps and statistics included in Appendix V present data for calcite, dolomite and total carbonate content.

The clay size fraction (<2 μm) of about 300-500 g of a 1 kg split of till samples was separated by centrifugation and decantation following the method of Lindsay and Shilts (1995). Approximately 1 g of the clay-sized fraction was analysed at Chemex Ltd. for a suite of trace and major elements using ICP-AES (inductively coupled plasma atomic emission spectrometry), following an aqua regia digestion (HCl-HNO_3, 3:1). Mercury was determined using CV-AAS (cold vapor atomic absorption spectrometry) after an aqua regia digestion for samples collected in 1996, 1997 and 1999. Aqua regia is a partial digestion that leaches organic matter, amorphous oxides, sulphides, and phyllosilicate minerals. Generally most base metals are dissolved with this extraction (Räisänen et al., 1992). Detection limits and analytical results are presented in Appendix VI for all till samples. Geochemical plots and statistics for elements with concentrations above detection limits in Class I and Class II till samples are included in Appendix VI.

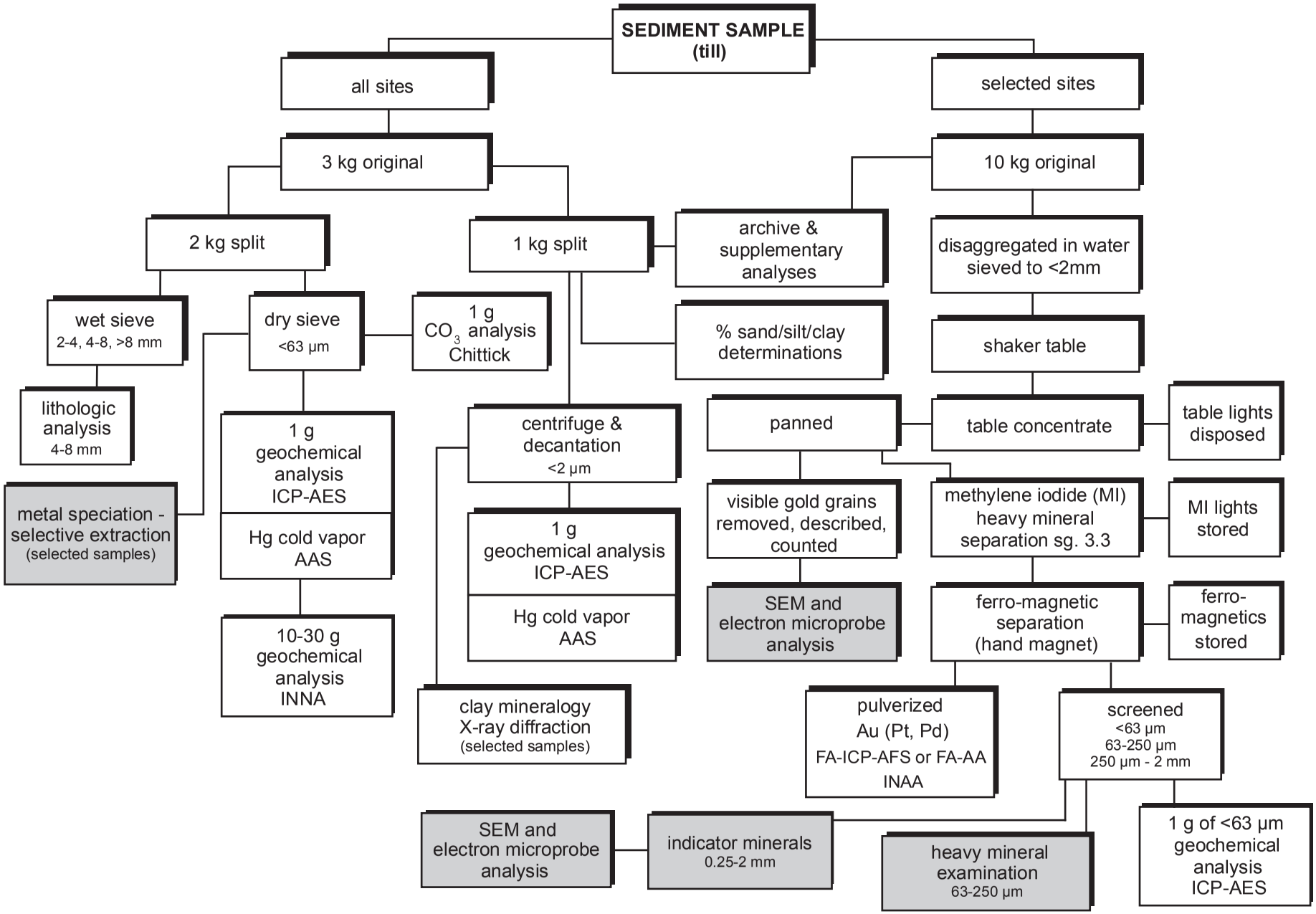

Figure 7. Flow diagram illustrating analytical scheme for till samples. Shaded boxes represent analyses that will be reported elsewhere.

About 1 g of the silt and clay size fraction (<63 μm) of till and esker sediment samples was analysed at Chemex Ltd. for a suite of trace and major elements using ICP-AES, following an aqua regia digestion. Mercury was determined using CV-AAS after an aqua regia digestion for samples collected in 1996 and 1997 only. Detection limits and analytical results are presented in Appendix VII for all samples. Geochemical plots and statistics for elements with concentrations above detection limits have been compiled for till samples (Class I and Class II) and esker sediment samples separately, and are included in Appendix VII.

About 10-30 g of the silt and clay size fraction (<63 μm) of till and esker sediment samples were analysed at Activation Laboratories Ltd. for Au and a suite of trace, major and rare earth elements using INAA (Instrumental Neutron Activation Analyses). Only Au, Sb, As and W were determined with this method for the 1999 samples. INAA provides total metal concentrations. Detection limits and analytical results are presented in Appendix VIII for all samples. Proportional dot maps and descriptive statistics for Au, As and Na concentrations have been compiled for till and esker sediment samples separately and are included in Appendix VIII. For comparisons of methods, Au concentrations determined by Fire Assay ICP-AFS (inductively coupled plasma atomic fluorescence spectrometry) for samples collected in 1996 and 1997, together with Pt and Pd values, are listed in Appendix IX.

The large bulk till samples and esker sediment samples were disaggregated and screened at 2 mm at Overburden Management Drilling Ltd. The <2 mm fraction was pre-concentrated with respect to density using a shaker table. Visible gold grains were recovered at the table and by panning of the remaining table concentrate, and subsequently counted and described with respect to morphology. Gold grains were <u>not</u> returned to the table concentrate but put into separate vials for further examination under the SEM. The table concentrate was then put in methylene iodide (specific gravity of 3.3) and the heavy mineral concentrate (HMC) was collected. After a ferromagnetic separation, half of the nonferromagnetic (NFM) concentrate was screened to recover the <63 μm, 63-250 μm and 250 μm-2 mm fractions. The fine fraction (<63 μm) of till samples was analyzed geochemically at Chemex Ltd. by ICP-AES, following an aqua regia digestion. Mercury was determined using CV-AAS after an aqua regia digestion. Detection limits and analytical results are presented in Appendix X. Maps included in Appendix X present data for several noteworthy elements for which values above the detection limit show a spatial pattern (As, Co, Cu, La, Ni, and Zn). The fine sand fraction (63-250 μm) was visually examined under the binocular microscope and

counted, and the coarse sand fraction (250 μm-2 mm) was analysed for indicator minerals. Results for those two fractions will be reported elsewhere. The other half of the NFM-HMCs of till and esker sediment samples was pulverized and analysed at Chemex Ltd. for Au, Pt and Pd by FA-ICP-AFS (1997 samples) and for Au by FA-AA and INAA (1998 samples). Geochemical results and detection limits are presented in Appendix XI. The total number of gold grains recovered, the weights of table feed, table pre-concentrates, NFM and ferromagnetic HMCs, and a detailed report on the gold grain count and classification are presented in Appendix XII. Proportional dot maps of the number of visible gold grains per 10 kg table feed and per NFM HMCs, and of NFM HMCs and magnetite per 10 kg table feed are included in Appendix XII.

About 300-500 g of the 1 kg split of all samples was used for textural analysis at the GSC Sedimentology Laboratory. The <2 mm (-10 mesh) fraction of bulk samples was separated by dry-sieving. The sand fraction (0.063-2 mm) was separated from the silt and clay fractions by dry-sieving (+ 230 mesh). The silt and clay fractions (-230 mesh) were determined with a Galai Particle Size Analyzer (PSA). The results were calculated as a percentage weight of the <2 mm fraction and are presented in Appendix XIII. Complete grain size distributions were determined with the PSA on a selection of samples and results are included in Appendix XIII.

Physical tests were completed on selected samples at the GSC Sedimentology Laboratory to determine various sediment properties. All results are compiled in Appendix XIV. Atterberg limits (Carter, 1993) could be determined on only three clay-rich marine samples. Nearly 50 other samples, mainly till and marine sands, were tested for Atterberg limits but most tests were incomplete because of high sand contents. Moisture contents and conductivity (Carter, 1993) were determined on small splits of selected large bulk till samples. pH was determined on the <2 mm fraction of selected bulk till samples and of till and humus samples collected in soil profiles (Knight et al., 2000). Loss-on-ignition, an approximation of total organic content, was done on the silt and clay size fraction (<0.063 mm) of selected 1997 till samples and on the clay size fraction (<0.002 mm) of 1999 till samples. Results for LOI are expressed as % weight loss of the dry weight after heating a small portion at 550°C for one hour (Sheldrick, 1984). Organic carbon was determined with a LECO Carbon Analyzer instrument on the silt and clay size fraction of 1998 and 1999 till samples and on the <2 mm fraction of humus samples collected in 1999 (Sheldrick, 1984). The remainder (<800 g) of all original (bulk) 3 kg and 10 kg samples was archived.

Quality Assurance and Quality Control (QA/QC)

Analysis of duplicate samples and analytical standards were used to monitor analytical precision and accuracy of geochemical results (e.g. Garrett, 1969, 1991). Analytical precision was assessed by inserting laboratory duplicate samples, i.e., samples prepared from the same field sample, but submitted with different sample numbers. No field duplicates were submitted. One duplicate in approximately 10 samples was submitted for analysis (8%). Precision was determined by first calculating the analytical variance (A^2) as follows (Garrett, 1969):

$$\mathbf{A^2} = \frac{1}{2N} \Sigma (X_{1i}-X_{2i})^2$$

Where A^2 is the analytical variance, X_{1i} is the sample analysis result, X_{2i} is the duplicate sample analysis result and N is the number of duplicate pairs. Logarithmic values were used only for the elements that had a range exceeding one order of magnitude (rf. Appendix XV). The precision was then computed (modified from Garrett, 1969):

$$\mathbf{RSD}\ (95\%\ \text{Confidence level}) = \frac{A \times 100\%}{X_{av}}$$

Where X_{av} is the average of all the replicate results. The value of Student's "t" was not used here therefore the precision is an estimate of the Relative Standard Deviation (RSD).

A single-factor fixed analysis of variance model can be used to determine if the analytical error is significantly smaller than the overall data variability (modified from Garrett, 1969). First the data variance was computed:

$$\mathbf{D^2} = \frac{1}{N-1} \Sigma (X_i-X_{av})^2$$

Where D^2 is the data variance, X_i is the average of each duplicate sample analysis result, X_{av} is the average of all the sample analysis results and N is the number of duplicate pairs. Again, log values were used only for the elements that had a range exceeding one order of magnitude. Then a variance ratio was determined:

$$\boldsymbol{F} = \frac{2 \times D^2}{A^2}$$

This ratio should exceed about 2 for 22 pairs of replicates and about 10 for 3 pairs (95%

Confidence level). The ratio rises as the number of replicates drops.

Analytical precision and variance ratios for elements above detection limits are compiled in Appendix XV. Laboratory duplicates were only inserted with samples analysed for trace and major element geochemistry. For the <0.002 mm fraction of till analysed by ICP-AES (rf. Appendix VI), the precision is very good for most elements, particularly for Al, Ba, Co, Cu, Fe, K, Mg, and Mn (<±5%). This method is less effective for Ca, Pb and Ti at low concentrations (>±10%), but appeared to be appropriate at higher levels. All variance ratios are high hence the data variability is much higher than the analytical error (*F*>15). Duplicate analyses of the <0.063 mm fraction of till samples (rf. Appendix VII) are generally as precise as for the clay fraction using the same method, and variance ratios are also high (*F*>5). Exceptions include As, Ba, Pb, Sc and Ti which are less precise than with the clay fraction. Pb analysis show particularly poor reproducibility (>±40%) because of low levels, and alternative analytical methods are suggested if better precision is required.

With the INAA method (rf. Appendix VIII), the analytical precision is poor for elements that occur in levels near the lower detection limit (Br, Ca, Cs, Mo, Sb, Ta, Tb and Zn) but generally good for all other elements. The method is less effective for Nd and U (>±15%) and relatively ineffective for Rb (±37% and *F*<2). Au analysis are poorly precise (±77%) for several reasons: 1) values close to lower detection limits in several duplicates, 2) relatively low sample weights (mean of 15 g), and 3) the particulate nature in which gold occurs coupled with sample inhomogeneity (the “nugget effect). However the variance ratio indicates that the precision is acceptable for Au considering the high data variability. Au anomalies are definitively questionable for sample weights below 5 g and resampling is required in those “anomalous” areas prior to further interpretation. For the analysis of the HMC <0.063 mm fraction of till (rf. Appendix X), the ICP-AES method is generally poorly precise, although only 3 replicate pairs were analysed so the precision may not be significant. Nevertheless, Ca, Co, Cu, Mg, Ni, P are much better with precisions below ±15%, and Co, Cu, Ni and P have high variance ratios (*F*>20).

Analytical accuracy was assessed by including GSC in-house control reference samples with the field samples. In every analytical batch, 2% standard samples were generally included. Analytical standards (i.e., TCA 8010) are monitored and maintained by the Terrain Sciences Division to ensure accuracy of data reported by the commercial laboratory. The mean of values

from previous analysis (<5 years) can be compared with the Meliadine results (Appendix XV). Results show that the accuracy is generally acceptable for all elements and for all methods as the Meliadine values are within two standard deviations of the mean of values from previous analysis. Exceptions include Ba, Sb and Sm concentrations analysed by INAA (<63 µm)and Au by FA-ICP-AFS, which are significantly higher than the average of the previous years results.

RESULTS AND DISCUSSION

Turbic cryosols are the prevalent type of mineral soils developed in glacial sediments of the Meliadine area. These soils are characterized by intense vertical mixing of material by frost heaving and churning. Relatively fresh bedrock fragments can be supplied to the soil and mixed in with oxidized drift and bedrock in areas of shallow bedrock, and/or organic matter recycled from the surface can be found throughout the active layer. C-horizons are therefore variably oxidized in the area, laterally and vertically, varying from relatively unoxidized to moderately oxidized. In mudboils where the material is extruded to the surface (Fig. 8), C-horizon samples are relatively homogenized and generally weakly weathered (Class I and II). Moreover, special care was taken not to include layers of organic material or heavily oxidized clasts (if present), and mudboils with little or no clasts on the surface or abundant shells were avoided (Class III samples).

Till matrix colour and texture

As indicated in Appendix II, the majority of till samples are greyish to olive brown (Munsell hue 2.5Y) and olive grey to olive (5Y) in colour, reflecting the incorporation of greenstone belt lithologies. The brownish grey to brown colored samples are also relatively common with either 2.5Y or 10YR hues. Those with 10YR hues are commonly the samples that are the richest in Dubawnt clasts.

Virtually all till samples collected in the region contain more than 5% gravel clasts (>2 mm) by weight (Appendix XIII). The average is 15%, varying from 1 to 37%, although the samples are not sufficiently large to produce useful statistics for gravel content. Over the map area, the till matrix (<2 mm) consists of 5 to 83% sand, 16 to 92 % silt, and 1 to 12% clay, with an average of about 52% sand, 46 % silt and only 2% clay. Variations in grain size distribution with depth are not significant. Over the study area, till derived from Archean gneiss and granites is sandier than till derived from greenstone belt lithologies. Thus, regionally, there appears to be a relationship

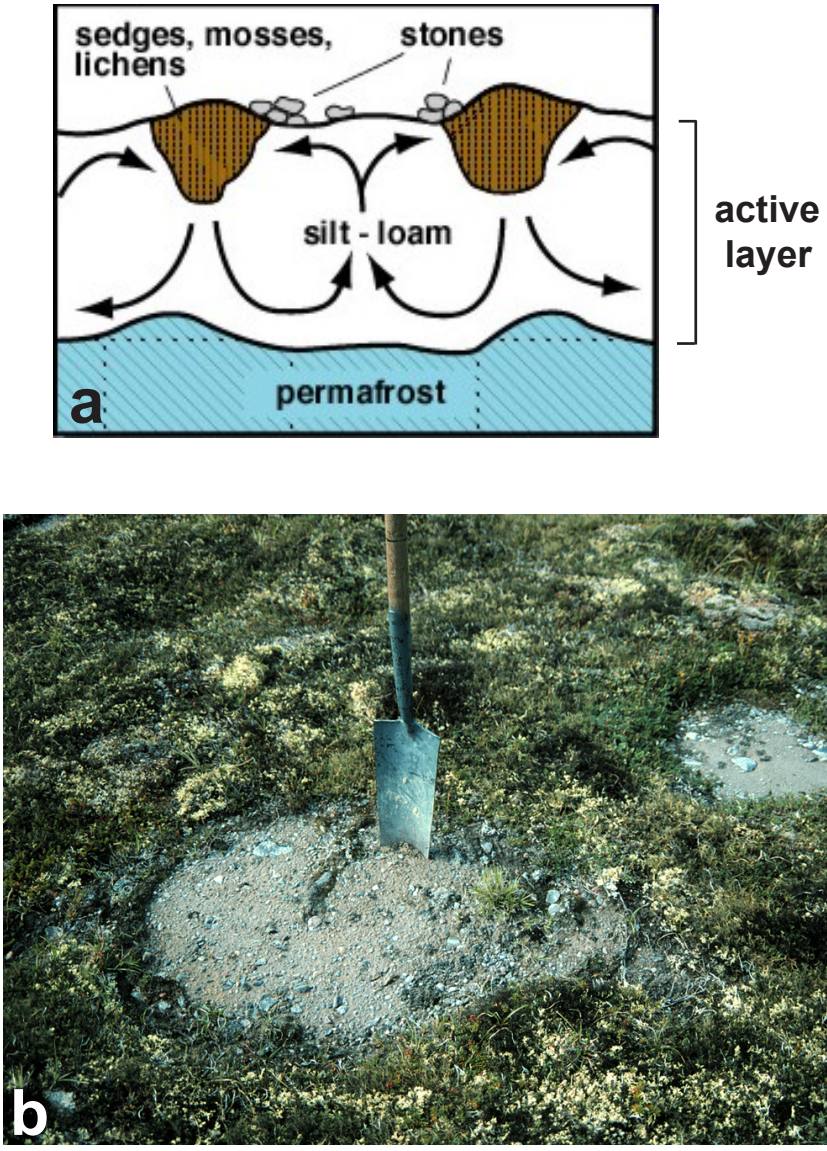

Figure 8. a) Simplified diagram of mudboil showing cryoturbation processes (from Levinson, 1980). b) Active mudboil with freshly extruded till in the centre surrounded by vegetation rim. Shovel is 15 cm wide.

between color and till lithology, and between grain size of till matrix and underlying bedrock type.

Till lithology

Lithological composition of the 4-8 mm pebble fraction of till presented in Appendix IV is characterized by: 1) intrusive and high grade metamorphic rocks (granitic) averaging 49% and ranging from 0 to 95%; 2) low grade metavolcanics and metasediments (greenstones) averaging 47% and ranging from 5 to 100%; 3) Dubawnts clasts averaging 4% and ranging from 0 to 22%; and 4) the absence of Paleozoic rocks. Regional variations are significant and are primarily related to the nature of up-ice lithologies and thickness of till sheet. For example, granitic clasts are predominant over intrusive/gneissic rocks outcropping northeast, north and southwest of the greenstone belt. Over the northwestern part of the greenstone belt where the drift is particularly thick (Peter Lake area), granitoid rich till is smeared across the greenstone terrain for more than 10 km down-ice from the source, indicating that (1) the coarse material in till is not renewed before a glacial transport distance of 10-20 km (i.e. >50% greenstones; Peltoniemi, 1985), (2) the first appearance of dispersal trains at the surface may well exceed 2 km in areas of thick till (Drake, 1983), and/or (3) the buried, approximate contact between the granitic terrain and the greenstone belt is inaccurate (Tella and Shau, 1994). Glacial dispersal of granitic rocks is also observed as far as 10 km down-ice from a large granitic intrusion north of Diana River where greenstone clast values are depressed relative to the rest of the greenstone belt. Nevertheless, high values of greenstone clasts in till are found throughout the belt (average of 56%), particularly in areas of thin drift (up to 100%), indicating that till lithology is closely related to the composition and nature of the local bedrock.

Dubawnt lithologies are most abundant in the SW part of the area (up to 22%), rapidly decreasing to near 0% towards the NE, forming the edge of the well known dispersal train of exotic red erratics from outcrops located 200 km up-ice (Fig. 4). Within the dispersal train, concentrations show a gentle, linear decrease in the direction of the last ice flow, which could reflect englacial transport with minimal modification of debris by crushing and abrasion, characteristic of dispersal by ice streams (i.e., Boulton, 1996; Dredge, 1995). However, the slow decay more likely represents the “tail” of the negative exponential curve of Krumbein (1937), characterized by glacial transport and abrasion as part of the basal debris load, as concentrations decrease exponentially in the direction of glacial transport from the source area down to the Meliadine Trend area

(McMartin and Henderson, 2000). Basal transport is also supported by the presence of locally derived stony till throughout the greenstone belt, even in areas of thick till, and a high ratio of greenstone belt clasts to Dubawnt clasts (average of 12). Outside the dispersal train, Dubawnt clasts are commonly absent but do occasionally occur in low concentrations (<2%). Dubawnt clasts in till have also been observed NE of the Meliadine Trend towards Chesterfield Inlet (T. Goodwin, pers. comm.). This contrasts with the "zero" Dubawnt south-east-trending line shown by Shilts et al. (1979) across the study area and interpreted as ice flow from the KID "throughout one or more glacial stades of the Wisconsinan Stage" (Shilts, 1980). The presence of occasional red erratics outside (NE) the dispersal train is significant in that it allows the concept that prior to the southeastward flow, a general easterly ice flow affected most of the area, an idea supported by the ice flow record (McMartin and Henderson, 1999).

Banded iron Formation (BIF) clasts occur in low concentrations averaging 0.22% in till and ranging from 0 to about 7%. However, any level of BIF in the pebble fraction usually indicates a close proximity to a known source. In some samples, the sulphide-bearing BIF clasts are intensively weathered hence actual levels are difficult to interpret in terms of glacial dispersal. The absence of carbonate Paleozoic clasts in till of the Meliadine area is interpreted as no ice flow from Hudson Bay. This refutes the idea of a long-term center of an ice sheet over Hudson Bay as modeled by Flint (1943), and later refuted by Shilts (1980). Distinct, buff colored, siliceous dolomite clasts are found in till near Rankin Inlet, but the source for these is undoubtedly Archean carbonates from Rankin Inlet Group outcrops located NW of town (Tella, 1994).

Till matrix mineralogy

The mineralogy of the till matrix (<2 mm) illustrates the local provenance of glacial sediments in the Meliadine area. Till is generally non-calcareous i.e. lacks a visible reaction to HCl in the field. Non-calcareous till generally contains 0 to 1% calcite, 0 to 0.5% dolomite and below 1.5% total carbonates according to the Chittick method (Appendix V). A few samples have a slight reaction to HCl but lack any significant (<1.5%) carbonates. On the other hand, samples showing a high reaction to HCl have no more than about 13.5% total carbonates. Values above 1.5% total carbonates indicate: 1) enrichment in calcite and/or dolomite along the coast from mixing of calcareous marine sediments in the active layer, 2) leaching and/or mixing of marine shells, 3) proximity to carbonate alteration associated to mineralization or to the Pyke Fault Zone, or 4) glacial transport of Archean carbonate lithologies. Partial or complete dissolution of carbonates

at depth resulting from the oxidation of till in the active layer, or precipitation of calcite at the surface, make carbonate values quite erratic. It is therefore apparent that calcite or dolomite concentrations do not correspond with carbonate pebble values.

The clay fraction (<2 μm) analyzed by X-ray diffraction consistently exhibits a prominent chlorite peak for greenstone-rich tills or a quartz and/or K-felspar peak for granite-rich tills. Plagioclase is abundant in all samples. Illite (biotitic) and amphibole are moderately abundant in the clay fraction and hematite is occasionally present. Traces of goethite and smectite were also found in two samples. No trace of kaolinite was found, including in the most Dubawnt-rich samples.

The light (s.g.<3.3), fine sand (63-250 μm) fraction is essentially composed of quartz (>90%). The heavy mineral (s.g.>3.3) fraction is dominated by hornblende, garnet *sp.* and epidote. Hematite, ilmenite and pyroxene *sp.* are moderately abundant. Fresh pyrite grains and pyrite coated with goethite were observed in about half of the samples examined under the microscope (up to 5.5% of 200 heavy minerals counted). The most abundant sulphides were found in till located directly down-ice from mineralization. Numerous sulphide grains were also observed in the coarser fraction of till (<2 mm) during pre-concentration of HMCs (rf. Appendix XII). The presence of labile minerals such as sulphides in surface till sampled above the permafrost table conflicts with the idea that sulphides are completely destroyed in the active layer (i.e., Shilts, 1977; Klassen, 1995). The cold climate and associated periglacial processes that bring relatively fresh sulphide-bearing bedrock fragments to the surface likely favour the preservation of some sulphide grains in till underlain by permafrost.

Till matrix geochemistry

Clay fraction

Data presented in Appendix VI include several regional trends in the geochemistry of the <2 μm fraction. In areas enriched with metal-poor granite debris, Al, Ba and K are generally high but most trace metal concentrations are suppressed. For example, a strong negative correlation exists between granitic clast content and As, Co, Cu, Fe and Ni concentrations. Inversely, these same trace metals, in addition to Pb and Zn, are relatively high in till enriched in greenstone clasts. Although the area underlain by the greenstone belt is one of high background for most metals, a few patterns of high abundances are consistent over three areas: 1) till near Rankin Inlet has

elevated Co, Cr, Cu, Fe and Ni values and this likely reflects the glacial comminution of serpentinite debris down-ice from ultramafic outcrops near the former Ni-Cu mine at Rankin Inlet (DiLabio and Shilts, 1977), and glacial dispersal from other Cu-Ni-Co occurrences in the area (Fig. 3); 2) till up-ice and down-ice from the eastern end of the Pyke Fault Zone has elevated Co, Cr, Cu, Fe, Mo, Ni, Pb and Zn concentrations, perhaps reflecting mineralization itself, the presence of ultramafic rocks along the Meliadine Trend, or glacial dispersal of kimberlitic rocks that have been reported from drill core, erratics and possibly outcrops in the general area (Miller et al., 1998; Seller, 1999; B. Kjarsgaard, pers. comm.); 3) zones of anomalous As, Co, Cu, Fe, Ni, Pb and Zn values occur in till over and down-ice from known gold mineralization and other potentially mineralized areas.

Fine-grained metal-bearing particles and grains of ore minerals are glacially comminuted and the elements redistributed into different grain sizes (Dreimanis & Vagners 1971). Furthermore, during weathering, it is evident that clastically dispersed labile minerals such as sulphides are partly decomposed in the oxidized active layer above the permafrost table (rf. Fig. 8a), releasing elements which are dissolved and transported by surface water. These elements preferentially accumulate in the clay-sized fraction (<2 μm) because clay minerals in this fraction have large surface area, high cation exchange capacity and can accommodate wide ranges of ionic radii (Shilts, 1995). In the clay fraction, most trace metals measured by ICP-AES after an aqua regia partial leach probably reside in primary phyllosilicates and secondary amorphous Fe-Mn oxides/hydroxides, and/or are adsorbed onto clay-size particles (Räisänen et al., 1992). This metal partitioning is demonstrated by the good correlation of most trace metals with Fe, Mg and Mn, and somewhat with Al and K, which are the main constituents of phyllosilicates and/or oxides/hydroxides. Exceptions include As and Pb, which do not correlate with any of the major elements nor with Mn, suggesting these elements partly reside within clay-sized sulphide particles and/or possibly fine-grained organic matter. More detailed chemical speciation studies have been undertaken on selected samples using selective extraction techniques to help determine in which phases the metals reside.

One other area of interest in terms of trace element distribution is within the Dubawnt clast dispersal train where Dubawnt values are relatively high (>10%). In this area, the exotic metal-poor Dubawnt debris slightly depresses the geochemical signature of the local bedrock, specifically Co, Cr, Fe, Mg, Ni and Zn concentrations. In contrast, Sr values are relatively high in the same area and show no correlation with Fe, Mg or Mn. Sr is a lithophile element that is concentrated in the earth's crust hence Dubawnt Supergroup lithologies, which include Proterozoic silicate rich

sedimentary rocks, are likely the source of the strontium. This is supported by high Sr values obtained on red Dubawnt bedrock samples analysed geochemically by ICP-MS (n=4, average = 303 ppm).

Silt and clay fraction

Data presented in Appendix VII for the geochemistry of the <63 µm fraction (ICP-AES) show regional trends that are similar to those for the <2 µm fraction, but values are significantly higher in the <2 µm fraction (2 to 25x). The <63 µm fraction contains predominantly silt-size minerals, and quartz is likely more important in this size range, acting as a diluting agent for trace elements. However, the correlation with most trace metals and Fe, Mg and Mn is still very good, if not better than with the clay fraction, suggesting most metals reside in or on clay-sized particles. Similar to the clay fraction, As, Pb, Sr and V do not correlate with Fe-Mg-Mn, and Sr values are generally higher in the Dubawnt dispersal train. One dissimilarity includes the poor correlation between Al or K with Mg-Fe-Mn in the <63 µm fraction, which may reflect the presence of more silt-size rock/mineral fragments, for example feldspar grains. P forms a distinct SE-trending dispersal train with concentrations higher outside the Dubawnt dispersal train. The glacial dispersal of silt-sized apatite group minerals, soluble in acid, from alkaline igneous rocks located up-ice from the greenstone belt is a likely source of phosphorous.

Results of geochemical analysis of the <63 µm fraction by INAA methods are presented in Appendix VIII. Most elements show similar patterns and near equal values from INAA relative to ICP analysis after an aqua regia digestion, particularly As, Co, Fe, La and Zn. The aqua regia digestion therefore represents near “total” concentrations for these elements. In contrast, INAA gives much higher Na values than with ICP (aqua regia), and a very distinctive pattern which was not seen with the ICP method is observed in the form of a SE-trending dispersal train outside the Dubawnt-rich till area. This perhaps reflects the glacial dispersal of resistant silt-sized Na-bearing silicates from granitic terrain up-ice from the greenstone belt. Ba is also much higher by INAA, as barite is not soluble in aqua regia, but no consistent patterns are observed with any of the two methods.

Gold and arsenic dispersal

Data for Au analysed by INAA in the <63 µm fraction of till (Appendix VIII) show that the area of highest concentrations is located along and down-ice from the Meliadine Trend near several

known showings and major occurrences. In this area, Au concentrations above the 75th percentile value (8 ppb) form a broad anomaly approximately 60 km long and 20 km wide. Three sites with Au concentrations in excess of 100 ppb are located within this anomaly. Although the general trend of the anomaly suggests glacial dispersal in the direction of the main regional ice flow event to the southeast, the extent of Au dispersal based on till geochemistry alone from 4 km spaced samples is difficult to determine. The presence of multiple sources, known and unknown, suggests the anomaly results from overlapping dispersal trains since most gold dispersal trains are known to be commonly short (<2 km) (i.e., Nichol et al., 1992). Similarly, although detailed sampling around the Discovery Zone indicates glacial transport distances exceeding 5 km for Au, a strong possibility remains that glacially transported Au-bearing sulphide-rich debris has been partly weathered out and that Au has been released locally at distances much farther than the original source, or that other unknown, buried sources are located immediately north of Atulik Lake.

Results for As analysed by INAA show that till along the Meliadine Trend has particularly high As concentrations, reflecting the abundance of arsenopyrite as one of the major sulphides in the auriferous oxide-iron formations and high-strain zones. Concentrations exceeding 9 ppm (50th percentile) are found in a 15 km wide anomalous zone extending to the ESE between Peter Lake and the coast. This anomaly is better defined than the broad Au anomaly. It roughly parallels the Meliadine Trend but concentrations do not regularly decrease in the direction of glacial transport. Again, glacial dispersal from multiple sources located along the Trend can explain this complex pattern. Glacial dispersal of As near Discovery indicates a long (>5 km) dispersal train down-ice from the zone, however, similar to Au, values are erratic within this train and actually increase north of Atulik Lake. Elevated As concentrations are also found in the southern part of the Rankin Inlet map area (55 K/16) where BIF erratics and clasts in the pebble fraction of till were occasionally found, and where gold concentrations are above the 75th percentile (8 ppb). The source for this anomaly is unknown.

The fairly good regional spatial correlation observed between As and Au is not observed on a site-to-site basis. The R^2 value on a linear correlation between Au and As in the <63 µm fraction (INAA) of till is only 0.36 (Figure 9). Gold analyses, however, generally exhibit lower reproducibility, which probably lowers the correlation. Most samples containing high As concentrations (>100 ppm) are anomalous with respect to Au in the <63 µm fraction whereas there are several samples with high Au but low As. This complex correlation likely reflects, in part, the

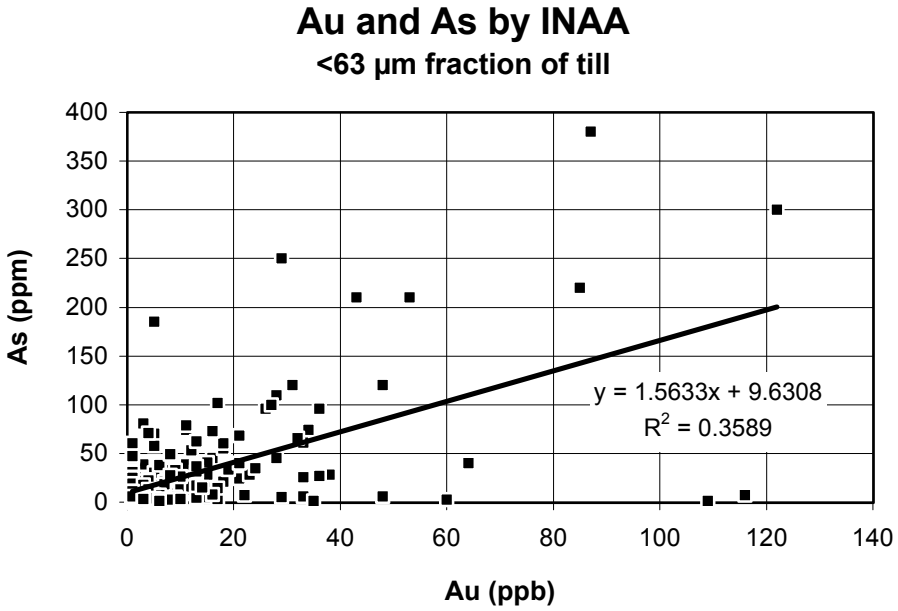

Figure 9. Au versus As in the <63 µm fraction of till samples (n = 289).

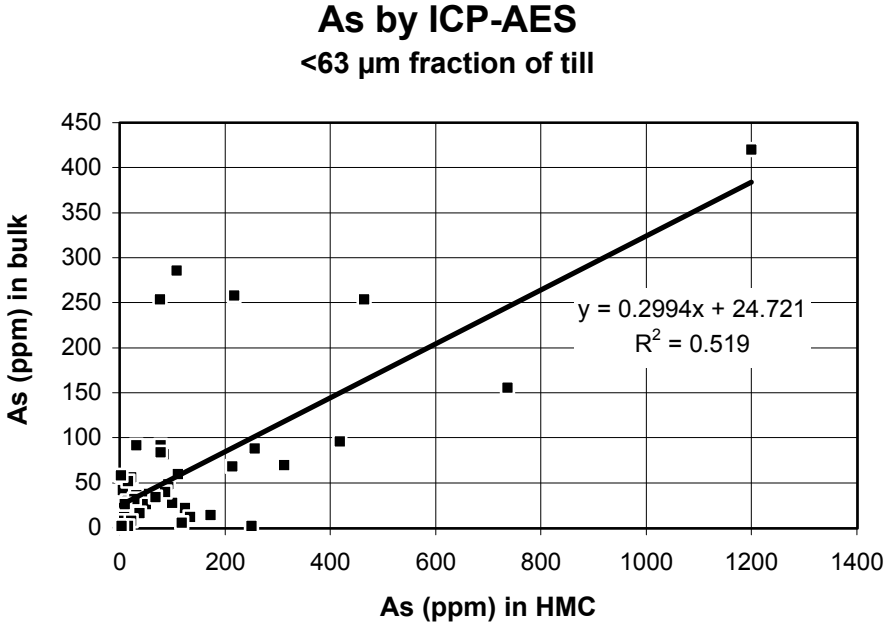

Figure 10. As in HMCs versus As in the <63 µm fraction of large till samples (n = 60).

lack of correlation between Au and As in mineralization.

In summary, factors such as differences in the age, primary form and grain size of Au in the two main types of mineralization (Miller et al., 1995; J. Kerswill, pers. comm.), and differences in glacial transport distances and possibly in the degree of sulphide weathering in the active layer appear to complicate the relationship between Au and As in till. It therefore appears that arsenic in till cannot be used directly as a pathfinder element for Au prospecting in the Meliadine Trend. Physical partitioning studies in selected samples will help to determine variations in fractionation of Au and As among the different styles of gold occurrences and the impact of glacial transport. The Au-As relationship in the HMC fraction and correlation with Au grain data will be discussed in the next sections.

Heavy mineral geochemistry

Data in Appendix X present results of geochemical analysis for the <63 µm non-magnetic heavy mineral concentrates (NFM-HMCs) of large till and esker sediment samples. No data on the mineralogy of this fraction are available but it is presumed that it closely resembles that of the 63-250 µm NFM-HMC fraction, hence, amphiboles, garnets, oxides, pyroxenes and some sulphides would predominate. Although the uneven distribution of large samples does not permit mapping of clear regional trends, most trace metals, for example As, Co, Cu, Ni and Zn (Appendix X), show elevated concentrations near known zones of mineralization. La is specifically elevated around the Discovery Zone. Trace elements are commonly equal or higher in the <63 µm bulk fraction (Al, Ba, Co, Cr, Cu, Mg, Ni, Sb, Ti and Zn) than in the HMC fraction, reflecting the concentrations of stable minerals in the finest fractions of till samples, such as phyllosilicates and hydrous oxides, as observed by Shilts (1973) in Keewatin. In contrast however, concentrations of several trace metals (i.e., As, Hg, Mo and Pb) are much higher in the heavy mineral suites than in the bulk till fraction. This confirms that metals held in labile minerals like sulphides, which are concentrated in the HMC, have not all been released by oxidation in the active layer. For example, As is 2 to 5x higher in the HMC than in the bulk fraction, and a fair relationship exists between As concentrations in both fractions (Figure 10), suggesting that an important part of the As in the <63 µm fraction of till may be held in As-rich sulphides.

Geochemical analysis of the <2 mm NFM-HMC fraction from which gold grains have been removed (Appendix XI) permits detection of gold encapsulated in sulphides, or more rarely, gold

not recovered during panning. Results show that some of the gold is present in sulphides as inclusions because the highest Au values in the heavy mineral fraction are found in till collected near mineralization. However, there is general lack of correspondence between Au in the HMC (<2 mm) and Au in the <63 µm bulk fraction of till (Fig. 11). This may reflect in part variations in the content of gold in different size fractions, but more likely that the bulk the Au occurs in particulate form in till. Although both As and Au in the heavy mineral fraction are generally highest near mineralization, the Au-As relationship (Fig. 12) is not much better than in the finest bulk till fraction, again reflecting indirect relations in terms of mineralized bedrock sources, form and grain size in till, and glacial dispersal.

Visible gold grains

Data presented in Appendix XII show the close correspondence between the number of gold grains in till and mineralization. The great majority of visible gold grains extracted from large bulk till samples were <60 µm in diameter (92%). Averill (in press) has published on the dominance of silt-sized gold in till and ores in Canada. The fine grained nature of Au in mineralization, and the fact that Au occurs largely in particulate form in till, is reflected in Figure 13 which shows a good relationship between gold grain counts and Au concentrations in the <63 µm bulk fraction of till. An average of 31 gold grains (70 grains/10 kg sample weight), ranging from 0 to 348 grains per till sample, were recovered. The highest counts (>25 grains/10 kg sample weight) occur within a narrow band (~ 5 km) that parallels the Meliadine Trend in between Atulik Lake and the southwest arm of Meliadine Lake. Within this band, a few sites close to mineralization have several large grains up to 300 µm in the long axis dimension. Gold grains classified through the binocular microscope using the scheme of DiLabio (1990) vary in morphology from pristine to reshaped. The highest proportion of pristine grains is in the silt size fraction (<50 µm), and although most grains are reshaped (66%), pristine grains generally occur within the Au grain anomalous area. However, the number of grains is probably the best indicator of closeness to deposit, as release of some pristine Au grains from sulphides is a strong possibility in weathered tills (Henderson and Roy, 1995), and probably in the active layer.

CONCLUSIONS

- Basal till over much of the Meliadine Trend is an appropriate sampling medium for gold prospecting. Till is abundant, locally derived and its provenance reflects a clear southeasterly direction of glacial transport.

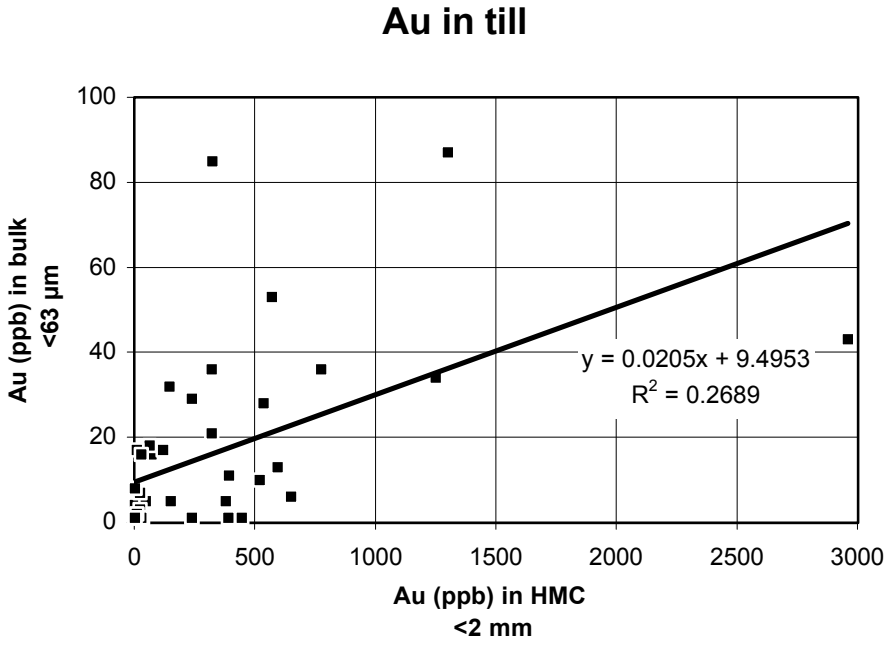

Figure 11. Au in HMCs (Fire Assay) versus Au in the <63 µm fraction (INAA) of large till samples (n = 42).

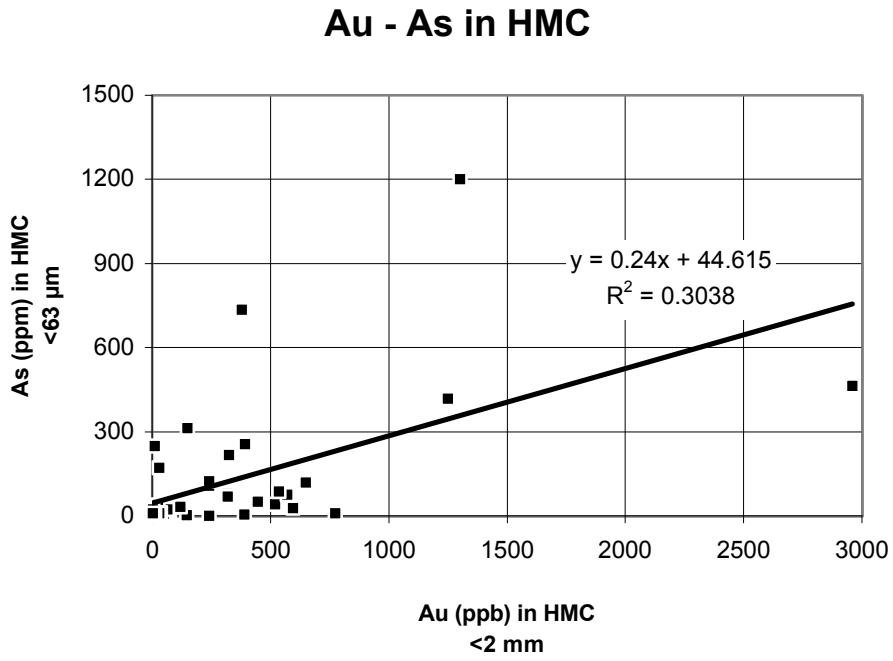

Figure 12. Au in HMCs (Fire Assay) versus As in HMCs (ICP-AES) of large till samples (n = 42).

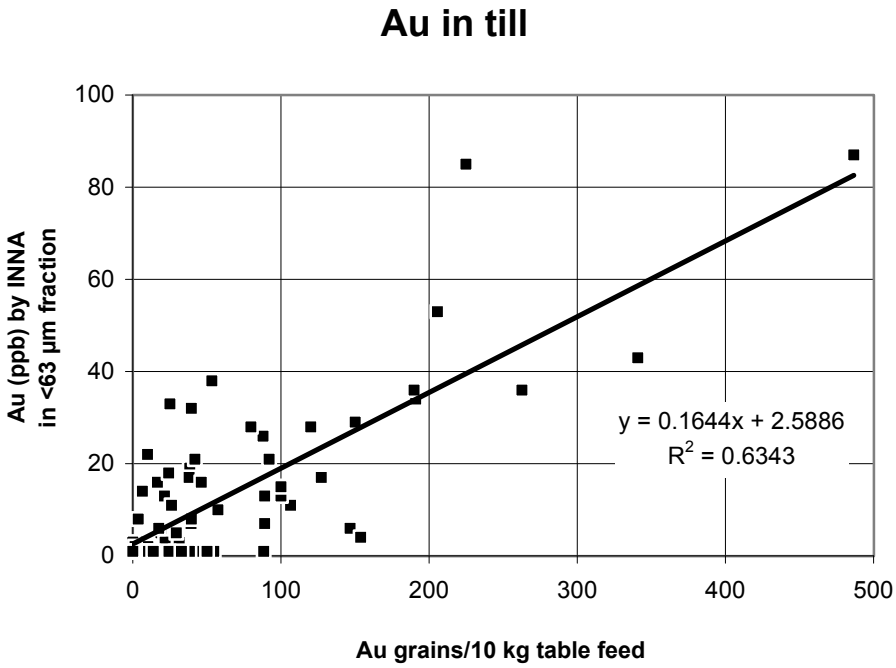

Figure 13. Number of Au grains per 10 kg of table feed of the <2 mm fraction versus Au in the <63 µm fraction of large till samples (n = 81).

- The seasonally thawed layer (active layer) in mudboils is analogous to the upper C-horizon layer above the water table in forested areas, hence till collected in mudboils at shallow depth is relatively unoxidized.

- The area has been influenced primarily by ice flowing to the southeast during the last glaciation. Lateral variations in surface till characteristics, and the lack of vertical variations, suggest samples were collected from the same till unit, i.e., having the same provenance from the northwest.

- The lithology of pebbles in till reflects the nature of sediment source and primary glacial processes. Marine reworking and redistribution has been minimal for most of the area. Till generally is locally derived, but thickness of glacial sediments is an important factor in controlling renewal distances.

- The presence of exotic Dubawnt-rich debris in the southwest half of the area does not significantly depress the local bedrock signature in till. The ratio of greenstone belt clasts to Dubawnt clasts remains high, with an average of 12.

- Till matrix mineralogy is characterized by a local provenance and the presence of sand-sized sulphide grains in low concentrations (<6 %) in HMCs of about half of the samples.

- Till geochemistry reflects both the glacial comminution of primary bedrock minerals and secondary accumulation in the finest fractions of till.

- The 4 km sample spacing exceeds the length of most Au dispersal trains but is useful to broadly define major features of sediment provenance and composition such as the Dubawnt dispersal train and associated Sr enrichments, Na and P dispersal from alkaline lithologies, and manifestations of gold mineralization zones along the Meliadine Trend (Au, As, Co, Cu, Fe, Ni, Pb and Zn).

- On a regional scale, the association of high As with high Au in dispersal trains supports the use of As to define Au-rich domains in till surveys. However, in the Meliadine Trend, the complex relationship observed between Au and As in mineralization, and particularly in till,

prevents the direct use of As in till as a pathfinder element for Au prospecting at the detailed scale.

- The bulk of the gold resides within the silt size fraction, forming a large (60 km long, >15 km wide) anomaly of values above the 75th percentile (8 ppb) along and down-ice from the Meliadine Trend. This anomaly represents the signature of overlapping dispersal trains from multiple known and unknown sources, hence Au glacial transport distances are difficult to determine with 4 km spaced samples.

- Most of the gold in the <63 µm fraction of till is due to gold grains, particularly free gold particulates. Some of the Au is also present as inclusions in sulphides in fresh till (<2 mm) collected in mudboils.

- An anomalous threshold of 25 grains/10 kg of sample weight can be used to define gold grain dispersal trains in till collected along the Meliadine Trend.

ACKNOWLEDGEMENTS

I am grateful to S. Khan and W. Carter for their enthusiasm and good companionship in the field. I wish to thank P. Lindsay and I. Girard for supervising the preparation of samples and analytical work, J. Percival for the time-consuming clay mineralogy analysis, and B. Garrett for discussions on QA/QC. I would also like to acknowledge Polar Continental Shelf Project for helicopter support. Field accommodations and logistical support at Discovery camp, Meliadine camp and Peter Lake camp were kindly provided by Cumberland Resources Ltd., WMC International Ltd. and Comaplex Minerals Corporation in 1997 and 1998. Thanks to K. Lauer for helping to prepare the Appendices. Ron DiLabio provided a thoughtful review.

REFERENCES

Armitage, A.E., Tella, S., and Miller, A.R., 1993. Iron-formation-hosted gold mineralization and its geological setting, Meliadine Lake area, District of Keewatin, Northwest Territories; *in* GSC Current Research 1993-1C, p. 187-195.

Averill, S.A., *in press*. The application of heavy indicator mineralogy in mineral exploration; *in* McClenaghan, M.B., Cook, S. and Bobrowsky, P.T. (eds.), Drift Exploration in Glaciated Terrain,

Geological Society of London, Special Volume.

Aylsworth, J.M., Kettles, I.M. and Shilts, W.W., 1981a. Surficial geology, Marble Island, District of Keewatin; GSC Map 10-1980, 1:125 000.

Aylsworth, J.M., Boydell, A.N. and Shilts, W.W., 1981b. Surficial geology, Tavani, District of Keewatin; GSC Map 9-1980, 1:125 000.

Aylsworth, J.M., Boydell, A.N. and Shilts, W.W., 1984. Surficial geology, Gibson Lake, District of Keewatin; GSC Map 1-1984, 1:125 000.

Boulton, G.S., 1996. Theory of glacial erosion, transport, and deposition as a consequence of subglacial sediment deformation; Journal of Glaciology, v. 42, p. 43-62.

Carpenter, R.L. and Duke, N.A., 1999. Geological setting of the lode gold deposits along the Meliadine Trend, Rankin Inlet greenstone belt, Nunavut; *in* Program & Abstracts of Talks and Posters, 27th Yellowknife Geoscience Forum, NWT Chamber of Mines, p. 10.

Carpenter, R.L. and Duke, N.A., 2000. Geological setting of gold deposits along the West Meliadine segment of the Pyke Break, Western Churchill Province, Nunavut; GeoCanada 2000, Conference CD, GAC, Calgary, June 2000.

Carter, M.R. (ed.), 1993. Soil Sampling and Methods of Analysis; Canadian Society of Soil Science, Ottawa, Canada, Lewis Publishers, CRC Press, p. 519-527.

DiLabio, R.N.W., 1990. Classification and interpretation of the shapes and surface textures of gold grains from till on the Canadian Shield; *in* GSC Current Research, Paper 90-1C, p. 323-329.

DiLabio, R.N.W. and Shilts, W.W., 1977. Detailed drift prospecting in the southern District of Keewatin; *in* GSC Current Research, Paper 77-1A, p. 479-483.

Drake, L.D., 1983. Ore plumes in till; Journal of Geology, v. 91, p. 707-713.

Dredge, L.A., 1995. Quaternary geology of northern Melville Peninsula, District of Franklin; Northwest Territories: surface deposits, glacial history, environmental geology, and till geochemistry; Geological Survey of Canada, Bulletin 484.

Dreimanis, A., 1962. Quantitative gasometric determination of calcite and dolomite by using Chittick apparatus; Journal of Sedimentary Petrology, v. 22, p. 125-145.

Dreimanis, A. and Vagners, U.J., 1971. Bimodal distribution of rocks and mineral fragments in basal tills; *in* Goldthwait, R.P. (ed.), Till - A Symposium, Ohio State University Press, Columbus, Ohio, p. 237-250.

Flint, R.F., 1943. Growth of the North American ice sheet during the Wisconsin age; Geological Society of America Bulletin, v. 54, p. 325-362.

Garrett, R.G., 1969. The determination of sampling and analytical errors in exploration geochemistry; Economic geology, v. 64, p. 568-574.

Garrett, R.G., 1991. The management, analysis and display of exploration geochemical data; *in* GSC Open File 2390, Paper 9, Exploration Geochemistry Workshop, March 1991, p. 9-1 to 9-41.

Henderson, P.J. and Roy, M., 1995. Distribution and character of gold in surface till in the Flin Flon greenstone belt, Saskatchewan; *in* GSC Current Research, Paper 1995-1E, p. 175-186.

James, R.S., DeSchutter, G.P., McDonald, A., Goff, S.P. and Armitage, A., 2000. Paragenesis of Au-arsenopyrite-pyrrhotite mineralization in banded, oxide facies iron formation, Meliadine Trend, Rankin Inlet greenstone belt, Nunavut; GeoCanada 2000, Conference CD, GAC, Calgary, June 2000.

Klassen, R.A., 1995. Drift composition and glacial dispersal trains, Baker Lake area, District of Keewatin, Northwest Territories; Geological Survey of Canada, Bulletin 485, 68 p.

Klassen, R.A. and Knight, R.D., 1996. Till geochemistry of the Baker Lake area, District of Keewatin, Northwest Territories; Geological Survey of Canada, Open File 3243.

Knight, R.D., LaPointe, M., Kyer, T., Henderson, P.J., 2000. Some observations on the effects of length of sample storage, sample type, and sample depth on the determination of pH in soils collected in the vicinity of the Horne smelter at Rouyin-Noranda, Quebec; *in* GSC Current Research, 2000-C24, 7p.

Krumbein, W.C., 1937. Sediments and exponential curves. Journal of Geology, v. 45, p. 577-601.

Levinson, A.A., 1980. Introduction to exploration geochemistry. The 1980 Supplement; Applied Publishing, Chicago, Illinois.

Lindsay, P.J. and Shilts, W.W. 1995. A standard laboratory procedure for separating clay-sized detritus from unconsolidated glacial sediments and their derivatives; *in* Drift Exploration, Borowsky, P.T., Sibbick, S.J., and Newell, J.M. (eds.), Journal of Geochemical Exploration, v. 21, p. 239-247.

McMartin, I. and Henderson, P.J., 1999. A relative ice-flow chronology for the Keewatin Sector of the Laurentide Ice Sheet, Northwest Territories (Kivalliq Region, Nunavut); *in* GSC Current Research, Paper 1999-C, p. 129-138.

McMartin, I. and Henderson, P.J., 2000. Till geochemistry as a tool for tracing mineral deposits in the Kivalliq Region, Nunavut; GeoCanada 2000, Conference CD, GAC, Calgary, June 2000.

Miller, A.R., Balog, M.J., and Tella, S., 1995. Oxide iron-formation-hosted lode gold, Meliadine Trend, Rankin Inlet Group, Churchill Province, Northwest Territories; *in* GSC Current Research, Paper 1995-C, p. 163-174.

Miller, A.R., Seller, M.H., Armitage, A.E., Davis, W.J., and Barnett, R.L., 1998. Late Triassic kimberlite magmatism, Western Churchill Structural Province, Canada; *in* Seventh International Kimberlite Conference Extended Abstract, p. 591-593.

Nichol, I., Lavin, O.P., McClenaghan, M.B., and Stanley, C.R., 1992. The optimization of geochemical exploration for gold using glacial till; Explor. Mining Geol., v.1, p. 305-326.

Peltoniemi, H., 1985. Till lithology and glacial transport in Kuhmo, eastern Finland; Boreas,

v.14, p. 67-74.

Räisänen, M.L., Tenhola, M. and Mäikinen, J., 1992. Effects of mineralogy and physical properties on till geochemistry in central Finland; *in* Bulletin of the Geological Society of Finland 64, Part I, p. 35-58.

Ridler, R.H. and Shilts, W.W., 1974. Exploration for Archean polymetallic sulphide deposits in permafrost terrains: an integrated geological/geochemical technique; Kaminak Lake area, District of Keewatin; GSC Paper 73-34, 33 p.

Seller, M.H., 1999. Petrology of the Meliadine kimberlite dykes, District of Keewatin, Northwest Territories, Canada; M.Sc. Thesis, University of Alberta, Spring 199, 227 p.

Sheldrick, B.H., 1984. Analytical methods manual, 1984; Research Branch, Agriculture Canada, LRRI Contribution no. 84-30.

Shilts, W.W., 1973. Drift prospecting; geochemistry of eskers and till in permanently frozen terrain: District of Keewatin; Northwest Territories; GSC Paper 72-45, 34 p.

Shilts, W.W., 1977. Geochemistry of till in perennially frozen terrain of the Canadian Shield - application to prospecting; Boreas, v. 6, p. 203-212.

Shilts, W.W.,1980. Flow patterns in the central North American ice sheet; Nature, v. 286 (5770), p. 213-218.

Shilts, W.W., 1995. Geochemical partitioning in till. *In* Drift Exploration in the Canadian Cordillera, Bobrowsky P.T., Sibbick S.J., Newell J.M. & Matysek P.F. (eds), British Columbia Ministry of Energy, Mines and Petroleum Resources, Paper 1995-2, p. 149-163.

Shilts, W.W. and Wyatt, P.H., 1989. Gold and base metal exploration using drift as a sample medium, Kaminak Lake - Turquetil Lake area, District of Keewatin; GSC Open File Report 2132.

Shilts, W.W., Cunningham, C.M. and Kaszycki, C.A., 1979. Keewatin Ice Sheet - Re-evaluation of the traditional concept of the Laurentide Ice Sheet; Geology, v. 7, p. 537-541.

Tella, S., Schau, M., Armitage, A.E., Seemayer, B.E., and Lemkow, D., 1992. Precambrian geology and economic potential of the Meliadine Lake-Barbour Bay region, District of Keewatin, Northwest Territories; *in* GSC Current Research Paper 92-1C, p.1-11.

Tella, S., 1994. Geology, Rankin Inlet (55K/16), Falstaff Island (55J/13) and Quartzite Island (55J/11), District of Keewatin, Northwest Territories, GSC Open File Map 2968, scale 1:50 000.

Tella, S., 1995. Geology, Scarab and Baird Bay, District of Keewatin, Northwest Territories; GSC Open File Map 3197, scale 1:50 000.

Tella, S. and Shau, M., 1994. Geology, Gibson Lake east-half, District of Keewatin, Northwest Territories; GSC Open File Map 2737, scale 1:250 000.

Tella, S., Annesley, I.R., Borradaile, G.J., and Henderson, J.R., 1986. Precambrian geology and parts of Tavani, Marble Island, and Chesterfield Inlet map areas, District of Keewatin: a progress report; GSC Paper 86-13, 20 p.

Tella, S., Eade, K.E., Sanford, B.V. and Okulitch, A.V. (compilers), 1997. Geology, Maguse River, District of Keewatin, Northwest Territories; GSC Map NP-15/16-G, scale 1:1 000 000.

Veillette, J.J., 1986. Former southwesterly ice flows in the Abitibi-Timiskaming region: implications for the configuration of the late Wisconsinan ice sheet; Canadian Journal of Earth Sciences, v. 23, p. 1724-1741.

Wright, G.M., 1967. Geology of the southeastern barren grounds, parts of the Districts of Mackenzie and Keewatin; GSC Memoir 350, 91 p.